RCS Measurements of a Human Hand for Radar-Based Gesture Recognition at E-band

Philipp Hügler, Martin Geiger, and Christian Waldschmidt
Ulm University, Institute of Microwave Engineering, 89081 Ulm, Germany
E-Mail: paul.huegler@uni-ulm.de

***Abstract*—This paper presents monostatic radar cross section (RCS) measurements of a human hand in the frequency range from 60 GHz to 90 GHz. These values are important parameters for system designs in the emerging field of radar-based gesture recognition. The measurement procedure is described in detail and results of four gestures at three different distances are depicted and analysed.**

I. Introduction

Radar is nowadays used in many different applications and is becoming present in everyday life. In the automotive industries, radar is used for advanced driver assistance systems such as forward collision warning (FCW) or adaptive cruise control (ACC) [1]. These sensors can also be used for pedestrian detection by investigating the Doppler spectrum, the range profile, and the signal-to-noise ratio [2]. In [3] not only the detection of humans, but also the classification of human activities is investigated. Based on micro-Doppler signatures, seven different activities (e.g. walking, crawling, and sitting) can be distinguished. Gesture recognition is gaining more and more interest, and mainly camera systems and optical depth sensors are used [4]. A multi-sensor system consisting of a colour camera, a depth camera, and a frequency modulated continuous wave (FMCW) radar is presented in [5]. A solely radar-based solution focusing on the evaluation of range-Doppler information is presented in [6]. Due to small physical dimensions and a growing number of available components, the 77 GHz band is promising for this type of application.

Evaluating design approaches for gesture recognition radar systems at 77 GHz requires a known RCS of a human hand. There are many publications dealing with the RCS of pedestrians at 77 GHz but only regarding the whole human body. According to [7] the frequency over azimuth average of a human wearing different kinds of clothes is suited between −7.7 dBsm to −3.0 dBsm. References dealing with the RCS of a human hand are not known to the authors. For a first estimation of an upper bound, a conducting metal sphere with the same radius r as a human fist (approximately 4 cm) is considered. The RCS under farfield condition ($d > \frac{2D^2}{\lambda}$, with d distance, D the maximum aperture, and λ the wavelength) is basically defined as the ratio of uniformly scattered power density $S_\mathrm{s}\left[\mathrm{W/m^2}\right]$ of a target to the incident power density $S_\mathrm{i}\left[\mathrm{W/m^2}\right]$ [8]

$$\sigma = 4\pi d^2 \frac{S_\mathrm{s}}{S_\mathrm{i}}. \tag{1}$$

Regarding a perfectly conducting sphere, its RCS mainly depends on frequency and radius. The frequency dependency is expressed by the circumference of a sphere normalised to the wavelength $\left(\frac{2\pi}{\lambda} r = kr\right)$. According to [8] the RCS in the geometric optic region $(kr > 10)$ can be approximated by its front face

$$\sigma_\mathrm{sphere} = \pi r^2. \tag{2}$$

In the other regions (Rayleigh and Mie region) the RCS varies a lot in a damped oscillating manner. Regarding the E-band (60 GHz to 90 GHz), kr is between 50 and 75. Under this condition, (2) can be applied and the upper bound of the RCS yields approximately −23 dBsm. Compared to the RCS of a human body, this value seems to be too high. Therefore, four gestures (fist, outstretched hand, palm, and back of the hand) at three different distances d (2.0 m, 1.5 m, and 1.0 m) are investigated.

II. Experimental Setup

In this section the measurement of a monostatic radar cross section is described. First, the used equipment and the geometrical arrangement is explained. Afterwards, the measurement procedure and the RCS calculation are detailed.

A. Measurement setup

In order to minimise disturbances caused by reflections of the surroundings, all measurements are carried out in an anechoic chamber with a size of $7\,\mathrm{m} \times 4\,\mathrm{m}$. Data is acquired using a vector network analyzer (VNA) and millimeter-wave converters to cover the whole E-band. Two identical standard gain horns (SGH) with $G_\mathrm{SGH} = 25\,\mathrm{dBi}$ gain and a 3 dB beamwidth of 7° are connected to the millimeter-wave converters using WR12 waveguides. All measurement equipment is placed outside the anechoic chamber and the millimeter-wave converters with the antennas are mounted at a peephole pointing into the chamber forming a bi-static radar configuration. As just the hand is of interest, an absorber wall with a width of approximately 1.6 m and a height of 2.4 m is placed in the anechoic chamber to cover the human body. The wall features a hole to put through an arm or calibration objects at a height of a human shoulder (ca. 1.5 m). Regarding the approximate length of a human arm with 0.6 m, the antennas are focused on a point 0.4 m in front of the wall and 1.5 m above the ground with the help of a laser rangefinder. The used equipment is listed in Table I and Fig. 1 shows an overview of the arrangement.

TABLE I. Overview of used measurement equipment.

Equipment	Model	Manufacturer
Vector network analyzer	ZVA50	Rohde & Schwarz
Millimeter-wave converter	ZVA-Z90E	Rohde & Schwarz
Standard gain horn	ARH-1225-02	Ducommun

ISBN 978-3-9812668-7-0

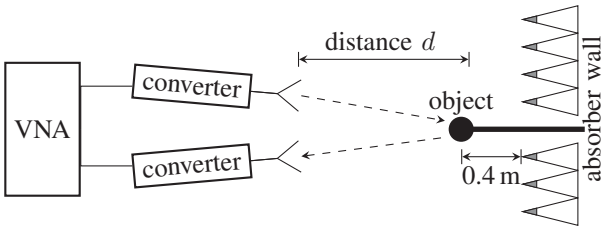

Fig. 1. Sketch of the used measurement setup using two frequency converters and standard gain horns.

B. Measuring procedure

In order to have a fixed reference point, a TRL (through, reflect, line) calibration using WR12 standards is performed at the interconnection of the SGHs and the millimeter-wave converters. The VNA settings are as follows:

Measurement bandwidth (RBW): 100 Hz

Number of points: 3001

For all regarded distances, firstly the backscatter of the empty chamber with absorber wall is measured and an inverse discrete Fourier transformation is applied using the VNA with a rectangular window. Fig. 2 depicts the time domain backscatter of the empty chamber with absorber wall as well as of a metal sphere with radius $r = 2.4\,\mathrm{cm}$ for distance $d = 2.0\,\mathrm{m}$. The noise floor is below $-130\,\mathrm{dB}$ and the sphere shows similar levels as the absorber wall. It can also be seen that no Tx/Rx coupling happens. Based on this figure, the stop time T_{stop} for time gating is determined. Regarding the number of measurement points and the covered frequency range, the ambiguity range Δt is 100 ns. Secondly, a time gate (Hann window) is applied from 0 ns to $T_{\mathrm{stop}} = 15\,\mathrm{ns}, 11\,\mathrm{ns}$, and $8\,\mathrm{ns}$ for $d = 2.0\,\mathrm{m}, 1.5\,\mathrm{m}$, and $1.0\,\mathrm{m}$ respectively, to eliminate unwanted backscatter. Comparing the maximum value of the time-gated backscatter of the chamber with absorber wall to the measured gestures and objects, a distance of at least 15 dB is given. Finally, the time-gated signal is transformed back to frequency domain. For RCS measurements a reference object with well-known RCS is needed. For all measurements a metal sphere with radius $r_{\mathrm{ref}} = 2.4\,\mathrm{cm}$ mounted on a wooden stick attached to the hole in the absorber wall is used as the reference object. The requirement for the optical region is fulfilled ($30 \leq kr_{\mathrm{ref}} \leq 45$) and (2) can be used to determine its RCS:

$$\sigma^{\mathrm{ref}} = 1.8 \times 10^{-3}\,\mathrm{m}^2 \widehat{=} -27.4\,\mathrm{dBsm}. \tag{3}$$

With the procedure explained above the time-gated forward voltage gain of the reference object S_{21}^{ref} is measured. Using the radar equation S_{21}^{ref} can be expressed as the ratio of the received power $P_{\mathrm{Rx}}^{\mathrm{ref}}$ and the transmitted power P_{Tx}:

$$\left|S_{21}^{\mathrm{ref}}\right|^2 = \frac{P_{\mathrm{Rx}}^{\mathrm{ref}}}{P_{\mathrm{Tx}}} = \frac{G_{\mathrm{SGH}}^2 \lambda^2}{(4\pi)^3\, d^4}\sigma^{\mathrm{ref}} = k_p \sigma^{\mathrm{ref}}. \tag{4}$$

Measuring another object or gesture yields to

$$\left|S_{21}^{\mathrm{obj}}\right|^2 = \frac{P_{\mathrm{Rx}}^{\mathrm{obj}}}{P_{\mathrm{Tx}}} = k_p \sigma^{\mathrm{obj}}. \tag{5}$$

By dividing (4) by (5), rearranging and expressing it in logarithmic form, the RCS of the object can be calculated as

$$\sigma^{\mathrm{obj}}\Big|_{\mathrm{dBsm}} = \left|S_{21}^{\mathrm{obj}}\right|\Big|_{\mathrm{dB}} - \left|S_{21}^{\mathrm{ref}}\right|\Big|_{\mathrm{dB}} + \sigma^{\mathrm{ref}}\Big|_{\mathrm{dBsm}}. \tag{6}$$

To validate the measurement procedure other objects with known RCS are used, e.g. corner reflectors and spheres of different sizes. For the distance $d = 1.0\,\mathrm{m}$ a second metal sphere with radius 1.25 cm is measured and the RCS is determined using (6). Fig. 3 depicts the result of the measured RCS σ^{meas}, the arithmetic mean, and the theoretical value (calculation based on series of Bessel functions [8]). Regarding the mean of the measured value as well as of the theoretical value, an amplitude offset of about 2.24 dB exists. Considering the 7° 3 dB beamwidth of the SGHs and the small distance of 1.0 m, the illuminated area is just 6.1 cm compared to the diameter of the reference sphere. The offset could therefore be caused by a small misalignment of the calibration sphere and is added to the measured gestures for $d = 1.0\,\mathrm{m}$.

III. Measurement Results

All four gestures considered for the measurement are depicted in Fig. 4. The photographs are taken from the peephole

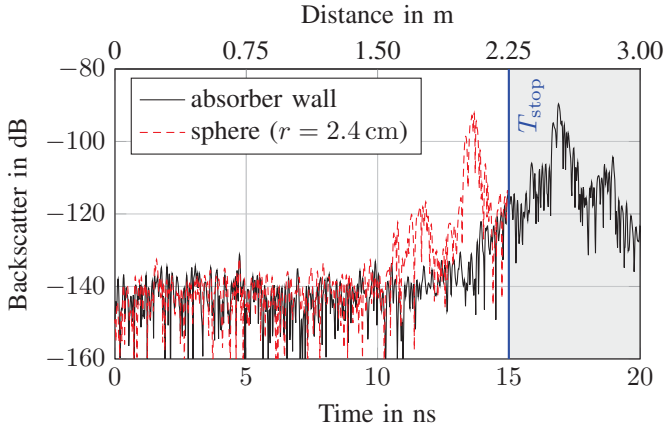

Fig. 2. Time domain backscatter of the anechoic chamber with absorber wall and a metal sphere with radius $r = 2.4\,\mathrm{cm}$ for distance $d = 2\,\mathrm{m}$.

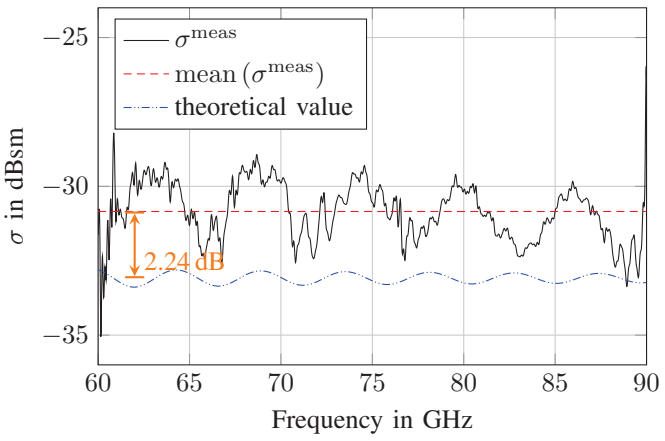

Fig. 3. Measured and theoretical RCS value of a metal sphere with radius $r = 1.25\,\mathrm{cm}$ and distance $d = 1.0\,\mathrm{m}$.

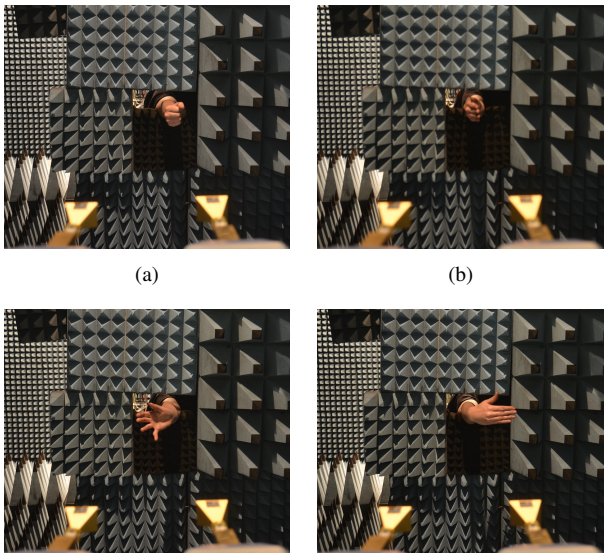

(a) (b) (c) (d)

Fig. 4. Photographs of the measured gestures, (a) fist, (b) outstretched hand, (c) palm, and (d) back of the hand for distance $d = 2.0\,\mathrm{m}$.

with the person behind the absorber wall putting his arm through the hole. The gestures namely fist, outstretched hand, palm, and back of the hand are chosen because with each imaginable hand movement one of these gestures will be occasionally present in front of a sensor. Measurements are carried out for all gestures stationary and for each distance d with the above explained measuring procedure and the corresponding RCS σ is calculated with (6). For better comparability, also the arithmetic mean of the measured RCS $\mathrm{mean}\,(\sigma)$ is considered. It is not possible to extract only the hand and, therefore, the measurements will be influenced by the arm. However, this is no drawback as in later applications an arm will also be present.

Fig. 5 (a) to (c) depict the results for a fist. For all three distances the characteristics of σ look quite similar. This is confirmed regarding the corresponding arithmetic mean ($-34.2\,\mathrm{dBsm}$, $-36.2\,\mathrm{dBsm}$, and $-35.5\,\mathrm{dBsm}$) which match good and differ by a maximum of 2.0 dB. As a human fist has not a simple geometry, ripples and notches occur caused by destructive interferences. Their position and deviation is sensitive to small movements of the arm (which could barely be suppressed), but the arithmetic mean keeps almost the same not differing more than 1.5 dB.

After investigating the fist, an outstretched hand gesture is analysed. It is expected that it has lower RCS values as the area facing the antennas is significantly smaller. The measurement results are plotted in Fig. 6 (a) to (c). As expected, the RCS is overall 5.0 dB lower and the arithmetic mean values for the distances are $-38.2\,\mathrm{dBsm}$, $-40.9\,\mathrm{dBsm}$, and $-41.9\,\mathrm{dBsm}$. The maximum deviation of the mean between the distances increases in comparison to the fist to 3.7 dB. The gesture itself is less plain and more spatially extended than the fist, hence the amount of ripple and notches caused by destructive interference are more dominant.

Next, the palm is measured. Since the area facing the antennas is increased compared to the fist and the outstretched hand, higher RCS values as for the fist are expected. Regarding

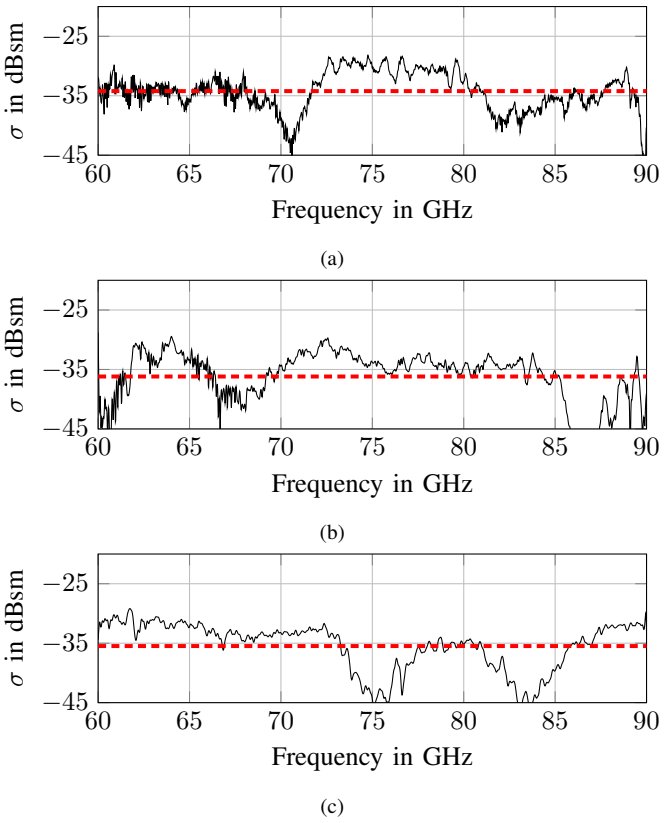

Fig. 5. Fist measurement: σ —— and $\mathrm{mean}\,(\sigma)$ - - - - for distance d (a) 2.0 m, (b) 1.5 m, and (c) 1.0 m.

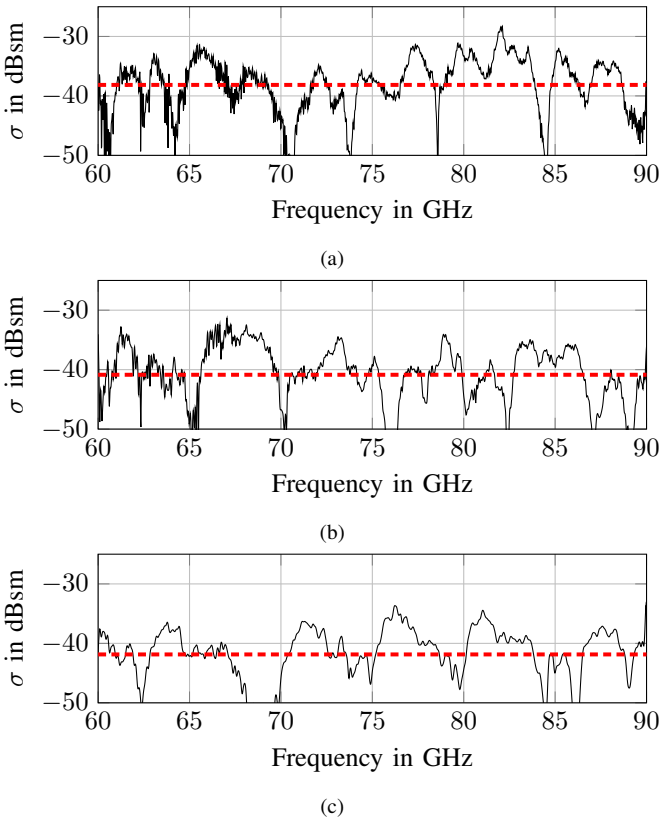

Fig. 6. Outstretched hand: σ —— and $\mathrm{mean}\,(\sigma)$ - - - - for distance d (a) 2.0 m, (b) 1.5 m, and (c) 1.0 m.

ISBN 978-3-9812668-7-0

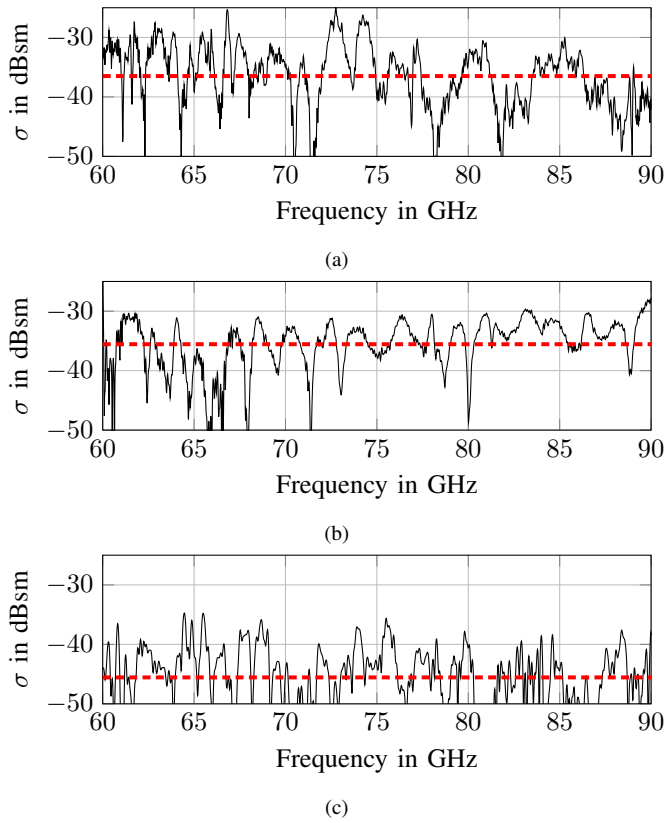

Fig. 7. Palm measurement: σ —— and $\mathrm{mean}\,(\sigma)$ ---- for distance d (a) 2.0 m, (b) 1.5 m, and (c) 1.0 m.

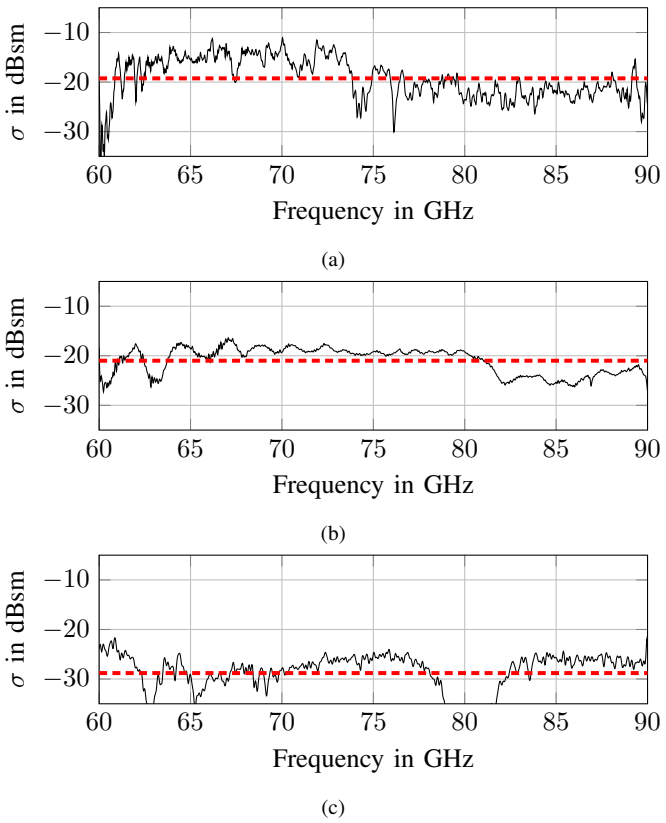

Fig. 8. Back of the hand measurement: σ —— and $\mathrm{mean}\,(\sigma)$ ---- for distance d (a) 2.0 m, (b) 1.5 m, and (c) 1.0 m.

the measurement results detailed in Fig. 7 (a) to (c), the mean values amount to −36.5 dBsm, −35.6 dBsm, and −45.6 dBsm respectively. For the distance $d = 1.0\,\mathrm{m}$ the RCS value and the corresponding mean drop dramatically by approximately 10 dB compared to the other distances. The reason is that for this distance the horn antennas do not illuminate the complete gesture because of their small 3 dB beamwidth. For $d = 2.0\,\mathrm{m}$ and 1.5 m the mean values match well. Neglecting the results for $d = 1.0\,\mathrm{m}$, the palm shows a slightly smaller RCS as the fist (about 1.0 dB).

For the back of the hand, as it has the plainest and largest geometry, the highest RCS value of all the considered gestures is expected. Regarding the measurement results in Fig. 8 (a) to (c), the arithmetic means are −19.3 dBsm, −21.0 dBsm, and −28.8 dBsm respectively, with the value for $d = 1.0\,\mathrm{m}$ again being significantly lower (about 9.0 dB). This is caused by the same reason as for the palm. The back of the hand for distance $d = 2.0\,\mathrm{m}$ and 1.5 m shows the smoothest response of all gestures, and nearly no notches with the highest overall RCS as expected. This can be explained by its already mentioned physical appearance.

IV. Conclusion

RCS measurement results for the four gestures fist, outstretched hand, palm, and back of the hand in the frequency range from 60 GHz to 90 GHz have been presented. It has been shown that the RCS of a human hand at these frequencies varies between −45 dBsm to −20 dBsm with the back of the hand having the highest and the outstretched hand the lowest RCS.

References

[1] J. Hasch, E. Topak, R. Schnabel, T. Zwick, R. Weigel, and C. Waldschmidt, "Millimeter-Wave Technology for Automotive Radar Sensors in the 77 GHz Frequency Band," *IEEE Transactions on Microwave Theory and Techniques*, vol. 60, no. 3, pp. 845–860, Mar. 2012.

[2] S. Heuel and H. Rohling, "Pedestrian Recognition in Automotive Radar Sensors," in *14th International Radar Symposium (IRS)*, vol. 2, Jun. 2013, pp. 732–739.

[3] Y. Kim and H. Ling, "Human Activity Classification Based on Micro-Doppler Signatures Using a Support Vector Machine," *IEEE Transactions on Geoscience and Remote Sensing*, vol. 47, no. 5, pp. 1328–1337, May 2009.

[4] S. Mitra and T. Acharya, "Gesture Recognition: A Survey," *IEEE Transactions on Systems, Man, and Cybernetics, Part C: Applications and Reviews*, vol. 37, no. 3, pp. 311–324, May 2007.

[5] P. Molchanov, S. Gupta, K. Kim, and K. Pulli, "Multi-sensor System for Driver's Hand-Gesture Recognition," in *11th IEEE International Conference and Workshops on Automatic Face and Gesture Recognition (FG)*, vol. 1, May 2015, pp. 1–8.

[6] Infineon Technologies. (2015, Jun.) Infineon and Google ATAP develop radar for gesture sensing and presence detection. [Online]. Available: http://www.microwavejournal.com/articles/24479-infineon-and-google-atap-develop-radar-for-gesture-sensing-and-presence-detection

[7] F.-G. J. C. Jean-Marc, *Radar Cross Section Measurements of Pedestrian Dummies and Humans in the 24/77 GHz Frequency Bands*. Publications office of the European Union, 2013. [Online]. Available: http://publications.jrc.ec.europa.eu/repository/handle/JRC78619

[8] E. F. Knott, J. F. Shaeffer, and M. T. Tuley, *Radar Cross Section*, 2nd ed. Broadstairs: Scitech, 2004.